

# Revisiting the ABC flow dynamo

Ismaël Bouya\*      Emmanuel Dormy†

February 3, 2019

## Abstract

The ABC flow is a prototype for fast dynamo action, essential to the origine of magnetic field in large astrophysical objects. We investigate its dynamo properties varying the magnetic Reynolds number  $Rm$ . We identify two kinks in the growth rate, which correspond respectively to an eigenvalue crossing and to an eigenvalue coalescence. The dominant eigenvalue becomes purely real for a finite value of the control parameter. Finally we show that even for  $Rm = 25000$ , the dominant eigenvalue has not yet reached an asymptotic behaviour and still varies significantly with the controlling parameter.

## 1 Introduction

We investigate the kinematic dynamo action associated with the well known ABC-flow (which stands for Arnold, Beltrami, Childress, see Dombre *et al.* (1986)). Its dynamo properties have been assessed in 1981 by Arnol'd *et al.* (1981) and it represents since then the prototype flow for fast dynamo action. A “fast dynamo” Childress and Gilbert (1995) is a flow which achieves exponential magnetic field amplification over a typical time related to the advective timescale and not the ohmic diffusive timescale (in which case it is referred to as a “slow dynamo”). The existence of fast dynamo action is essential to account for the presence of magnetic field in astrophysical bodies, for which the ohmic diffusive time is often larger than the age of their formation. If self-excited dynamo action is to account for their magnetic field, it is therefore essential that it be achieved over an advective timescale. The most classical flow to exemplify such “fast dynamo” action is indeed the ABC-flow. Arnold and Korkina (1983) first investigated the dynamo property of the ABC-flow, originally introduced to investigate Lagrangian chaos. Many developments followed, which will be dicussed in the course of this article. Galloway and Frisch (1984, 1986, 1987)

---

\*UMR 7586 Institut de mathématiques de Jussieu – Analyse fonctionnelle  
ismael.bouya@normalesup.org

†MAG (ENS/IPGP), LRA, Département de Physique, Ecole Normale Supérieure, 24, rue Lhomond, 75231 Paris Cedex 05, France.  
dormy@phys.ens.fr

## 2 Numerical method

We are concerned with the kinematic dynamo problem, for which a solenoidal magnetic field evolution is governed under a prescribed flow by the induction equation

$$\frac{\partial \mathbf{B}}{\partial t} = \nabla \times (\mathbf{u} \times \mathbf{B} - \text{Rm}^{-1} \nabla \times \mathbf{B}) . \quad (1)$$

We consider here the ABC-flow (Arnold (1965); Henon (1966)), which takes the form

$$\mathbf{u} = (A \sin z + C \cos y) \mathbf{e}_x + (B \sin x + A \cos z) \mathbf{e}_y + (C \sin y + B \cos x) \mathbf{e}_z, \quad (2)$$

and restrict our attention to the case where the magnetic field has the same periodicity as the flow (i.e.  $2\pi$ -periodic in all directions of space, see Archontis, Dorch, and Nordlund (2003) for extensions) and the weight of the three symmetric Beltrami components are of equal strength ( $A = B = C \equiv 1$ ).

Let us stress again that we also restrict our attention to the kinematic dynamo problem, in which the flow is analytically prescribed and unaltered by the magnetic field (see Galloway and Frisch (1987) for an investigation of the stability of this flow).

The choice  $A : B : C = 1 : 1 : 1$  yields very small chaotic regions and is thus non optimal for dynamo action (see Alexakis (2011) for a detailed study of this point), it however corresponds to the largest symmetry class for this kind of flows, and has for this reason been intensively studied.

The simulations presented in this article were performed using a modified version of a code originally developed by Galloway and Frisch (1984) and which uses a fully spectral method with explicite mode coupling.

The original time-stepping used by Galloway and Frisch (1984) relies on a Leapfrog scheme stabilized by a Dufort-Frankel discretization of the diffusive term. Introducing  $\mathcal{L}$  to denote the discretized diffusion operator, which is local in Fourier space, and  $\mathcal{NL}$  to denote the discretized inductive term, non-local as it couples neighboring modes, this scheme can be expressed as

$$\mathbf{B}^{n+1} = \mathbf{B}^{n-1} + 2dt \left( \mathcal{NL}(\mathbf{B}^n) + \frac{1}{2} \mathcal{L}(\mathbf{B}^{n+1} + \mathbf{B}^{n-1}) \right), \quad (3)$$

using a red-black (or Chlorite-Sodium) staggering in time and space, see Galloway and Frisch (1986).

We have implemented two alternative time stepping schemes, in order to assess the stability of the temporal evolution at large values of  $\text{Rm}$ . We used a Crank-Nicholson Adams-Bashforth scheme

$$\mathbf{B}^{n+1} = \mathbf{B}^n + dt \left( \frac{1}{2} \mathcal{L}(\mathbf{B}^{n+1} + \mathbf{B}^n) + \frac{3}{2} \mathcal{NL}(\mathbf{B}^n) - \frac{1}{2} \mathcal{NL}(\mathbf{B}^{n-1}) \right), \quad (4)$$

as well as a second order BDF discretization

$$\frac{3}{2} \mathbf{B}^{n+1} = 2 \mathbf{B}^n - \frac{1}{2} \mathbf{B}^{n-1} + dt \left( \mathcal{L}(\mathbf{B}^{n+1}) + 2 \mathcal{NL}(\mathbf{B}^n) - \mathcal{NL}(\mathbf{B}^{n-1}) \right). \quad (5)$$

These two schemes are unstaggered and involve larger memory requirements, still offering the same complexity. All schemes are semi-implicite, but retain an explicite marching for the non-local term in order to prevent the resolution of a linear system at each timestep. We verified that the results presented in this article are independant of the above choices.

The computing time obviously varies with the control parameter  $\text{Rm}$ . If all spatial modes are computed up to a truncation  $N$ , the computational complexity scales like  $\mathcal{O}(N^4)$ . Assuming the asymptotic scaling of the magnetic field lengthscale, we get  $N \sim \text{Rm}^{1/2}$  and thus expect a complexity growing as  $\mathcal{O}(\text{Rm}^2)$ . We have therefore derived a parallel version of the code using the MPI library and a spectral domain decomposition strategy to tackle larger values of  $\text{Rm}$ . This yields shorter computing time at large resolution.

The results presented in this article were obtained with numerical resolutions ranging from  $N = 64$  for the smallest values of  $\text{Rm}$  to  $N = 1024$  for  $\text{Rm} = 25000$ . In all cases we verified that the results reported here were unaltered by doubling the resolution.

It is worth stressing that the quantity  $\nabla \cdot \mathbf{B}$  is obviously preserved by (1), and that this essential property is retained by the discrete numerical schemes, and thus the magnetic field remains solenoidal throughout the simulations.

We investigate a linear problem and therefore expect that, independantly of the initial conditions, the long time integration will simply reflect the eigenmode with largest growth rate (unless the initial condition happened to be orthogonal to this mode). In practice, we used the same initial condition as in the earlier studies, i.e.

$$\mathbf{B}(t = 0) \propto (\sin z - \cos y) \mathbf{e}_x + (\sin x - \cos z) \mathbf{e}_y + (\sin y - \cos x) \mathbf{e}_z. \quad (6)$$

### 3 Modes crossing

Figure 1 presents the evolution of the maximum growth rate of the magnetic field as a function of  $\text{Rm}$ . Each point on the figure corresponds to a three-dimensional simulation. We confirm growth rates obtained by earlier studies (see Galloway (2012) for a recent review), and we extend the range of investigation from  $\text{Rm} < 1600$  to  $\text{Rm} < 25000$ . The curve has been validated against published growth rates using spectral methods Galloway and Frisch (1986); Lau and Finn (1993) as well as a finite volume method Teyssier, Fromang, and Dormy (2006) for which simulations have been performed up to  $\text{Rm} = 2000$  (Teyssier & Dormy private comm.).

In addition to the wider extend of  $\text{Rm}$  variation, the curve also offers a finer resolution than previously obtained graphs. This highlights the presence for two kinks in the curve, labeled  $\text{Rm}_1$  and  $\text{Rm}_2$  on the figure. The first of these occures in the stable window reported by Galloway and Frisch (1986) near  $\text{Rm} = 20$  and corresponds to  $\text{Rm}_1 \in [24.6, 25.1]$ . A mode crossing was previously suggested owing to the changes in the eigenfunction symmetry Galloway (2012). Here we demonstrate this eigenvalue crossing by following both eigenvalues on each side of the crossing. In fact whereas time stepping algorithm usually only provide information on the dominant eigenvalue, i.e. the eigenmode with largest growth rate, we use it here to get more information. Indeed, transient behavior starting with well selected initial conditions provide information on the behavior of a given mode, even if it is not the dominant eigenmode (see

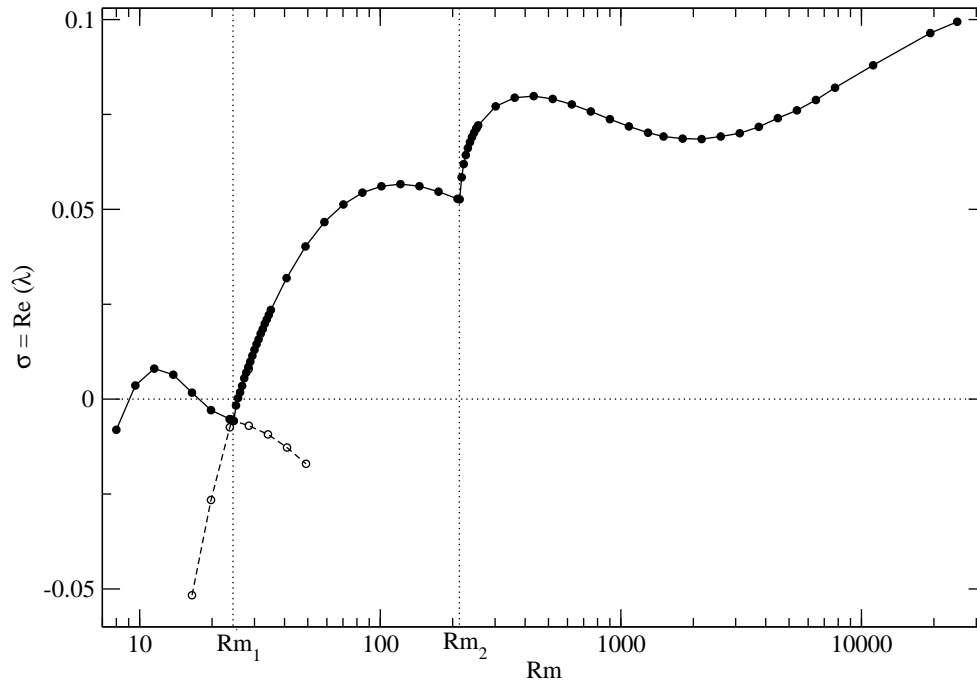


Figure 1: Plot of the real part of the eigenvalue for the fastest growing magnetic field mode as a function of the magnetic Reynolds number  $Rm$  (using logarithmic scale in the  $x$ -axis).

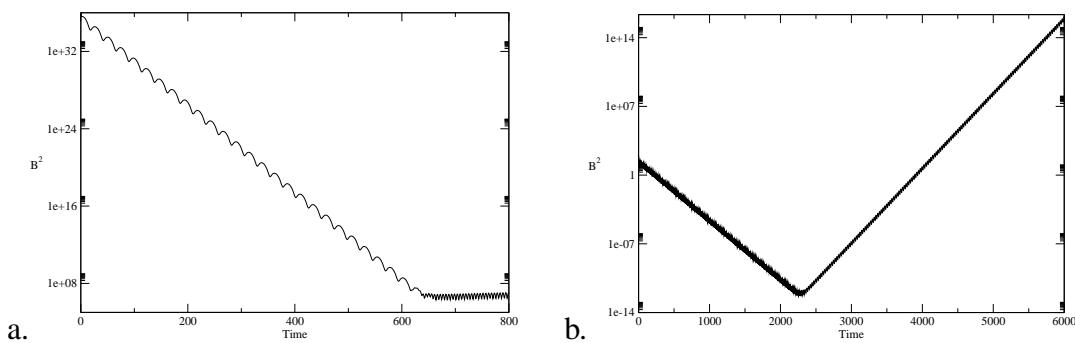


Figure 2: Time evolution of the magnetic energy, which highlights the information provided by transient behaviors. Left (a) a simulation for  $Rm = 16.5 (< Rm_1)$  using as initial condition the final solution obtained at  $Rm > Rm_1$ , right (b) simulation for  $Rm = 28.4 (> Rm_1)$ .

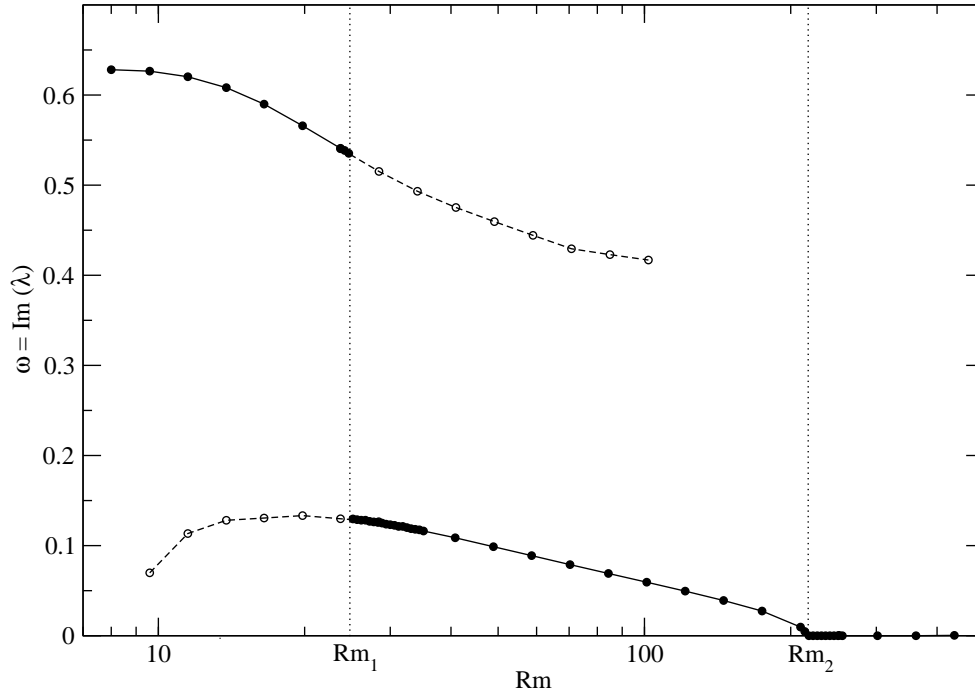


Figure 3: Plot of the imaginary part of the eigenvalue as a function of  $Rm$  (using logarithmic scale in the  $x$ -axis).

Figure 2). This transient behavior allowed us to continue the branches corresponding to each eigenvalue outside of the region in which they are dominant eigenvalues (see dotted lines and open symbols on Figure 1).

As noted by earlier authors, the eigenvalues are complex, leading to oscillations of the energy, visible on Figure 2 (particularly on the first part of Figure 2a, as the period of oscillations is elsewhere very short compared to the time extend of the plot). The imaginary part of the dominant eigenvalue  $\omega = \text{Im}(\lambda)$  can thus be directly determined from these time series. The graph  $\omega(Rm)$  is displayed on Figure 3. As explained above, not only do we display the dominant eigenvalue (solid line and symbols) but we are also able to follow each mode past their region of selection (dotted lines and open symbols). One can note that, as  $Rm$  increases past  $Rm_1$ , the imaginary part of the dominant eigenvalue jumps discontinuously from  $\omega \simeq 0.53$ , corresponding to the first window identified by Arnold and Korkina (1983), to  $\omega \simeq 0.13$  corresponding to the second window of Galloway and Frisch (1986). This discontinuous jump in the pulsation highlights the eigenvalue crossing occurring at  $Rm_1$ . There again, transient behaviors were used to obtain the open symbols.

## 4 Eigenvalues coalescence

As the magnetic Reynolds number is further increased, a second kink in the growth rate is observed on Figure 1 for  $Rm_2 \in [215.0, 215.4]$ . This second accident, however, does not correspond

to a change of dominant eigenvalue, but instead to an eigenvalues coalescence. The strategy highlighted above to follow secondary modes is inefficient here, indicating that there is no significant change in the dominant eigenmode.

Figure 3 reveals that the behavior of the imaginary part of the eigenvalue is very different near the second kink. Instead of the abrupt jump reported at  $\text{Rm}_1$ , the pulsation continuously tends to zero as  $\text{Rm}$  approaches  $\text{Rm}_2$  and vanishes for  $\text{Rm} > \text{Rm}_2$ .

The lack of oscillations at large  $\text{Rm}$  is a well known characteristic, it was already noticed by Galloway and Frisch (1984) for ( $\text{Rm} > 400$ ), although they could not assess whether the period of oscillations was simply increasing with  $\text{Rm}$  or the eigenvalue had become purely real. Lau and Finn (1993) suggested that this could be associated with a mode crossing, a new mode with purely real eigenvalue taking over above  $\text{Rm}_2$ .

We show here that the imaginary part of the eigenvalue indeed vanishes for  $\text{Rm} > \text{Rm}_2$ , and that this corresponds to the coalescence of two complex conjugate eigenvalues on the real axis. The coalescence yields the kink in the evolution of the real part of the eigenvalue.

The simplest mathematical model for a complex conjugate eigenvalue coalescence on the real axis corresponds to a situation of the form

$$\lambda_{\pm} = \alpha(\text{Rm}) \pm \sqrt{\beta(\text{Rm})}, \quad (7)$$

where  $\alpha$  and  $\beta$  are differentiable real functions of  $\text{Rm}$ . A negative  $\beta$  (for  $\text{Rm} < \text{Rm}_2$ ) yields two complex conjugate modes, and thus oscillations of the magnetic energy. As  $\beta$  becomes positive (for  $\text{Rm} > \text{Rm}_2$ ), the eigenvalues are purely real and the  $\beta$  term now contributes to the real part of the eigenvalue  $\lambda_+$  offering the largest growth rate.

Figure 4.a presents a detailed view on the variation of  $\sigma = \text{Re}(\lambda)$  and  $\omega = \text{Im}(\lambda)$  close to  $\text{Rm}_2$ . Defining  $\sigma_2 = \sigma(\text{Rm}_2)$  we plot  $\sigma(\text{Rm}) - \sigma_2$  and  $-\omega(\text{Rm})$ . It is clear that the kink in  $\sigma$  is concomitant of the vanishing of  $\omega$ .

Let us now form on Figure 4.b the quantity  $F = \sigma(\text{Rm}) - \sigma_2 - \omega(\text{Rm})$ . The square-root behavior of  $F$  near  $\text{Rm}_2$  is obvious. Assuming that the above model (7) is correct,  $F$  corresponds to  $\alpha - \alpha_0 + \text{sign}(\beta) \sqrt{|\beta|}$ , where  $\alpha_0 = \alpha(\text{Rm}_2)$ . We can note on Figure 4.a for  $\text{Rm} < \text{Rm}_2$  that  $\alpha - \alpha_0$  remains small compared to variations in  $\beta$ . The quantity  $\text{sign}(\text{Rm} - \text{Rm}_2) F^2$  therefore offers a good approximation to  $\beta$  and should be differentiable at  $\text{Rm}_2$ .

More formally, assuming that  $\alpha$  and  $\beta$  are regular functions of  $\text{Rm}$ , we can write a finite expansion of the form

$$\alpha = \alpha_0 + \alpha_1(\text{Rm} - \text{Rm}_2) + \alpha_2(\text{Rm} - \text{Rm}_2)^2 + \dots, \quad (8)$$

$$\beta = \beta_1(\text{Rm} - \text{Rm}_2) + \beta_2(\text{Rm} - \text{Rm}_2)^2 + \dots, \quad (9)$$

with  $\beta_1 > 0$ . The quantity  $\text{sign}(\text{Rm} - \text{Rm}_2) F^2$  can be written at the lowest orders in  $\text{Rm} - \text{Rm}_2$

$$\begin{aligned} \text{sign}(\text{Rm} - \text{Rm}_2) F^2 &= \text{sign}(\text{Rm} - \text{Rm}_2) \alpha_1^2 (\text{Rm} - \text{Rm}_2)^2 \\ &\quad + \text{sign}(\text{Rm} - \text{Rm}_2) \alpha_1 \sqrt{\beta_1} (|\text{Rm} - \text{Rm}_2|)^{3/2} \\ &\quad + \beta_1 (\text{Rm} - \text{Rm}_2). \end{aligned} \quad (10)$$

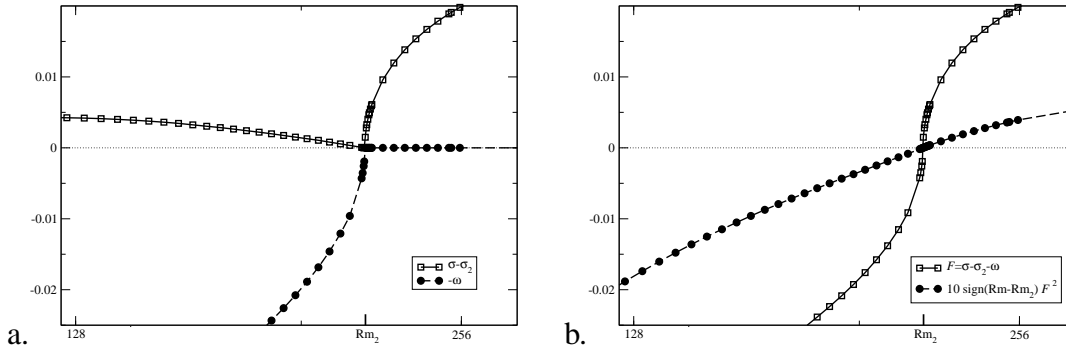


Figure 4: Eigenvalues coalescence for  $Rm$  close to  $Rm_2 \simeq 215$ . Both the real part (written as  $\sigma(Rm) - \sigma_2$ ) and the opposite of the imaginary part (i.e.  $-\omega(Rm)$ ) are represented (a). The sum  $F$  of both (b), and  $\text{sign}(Rm - Rm_2)F^2$  illustrate the continuity and regularity in the functional form of the eigenvalue (see text).

This development implies that  $\text{sign}(Rm - Rm_2)F^2$  is differentiable at  $Rm_2$ . Figure 4.b clearly illustrate this property on the direct numerical simulation.

We observed no significant changes in the eigenmode after the eigenvalues coalescence. Indeed the “double cigars” structure (see Dorch (2000)), associated to the oscillations for  $Rm \in [Rm_1, Rm_2]$  is preserved once the growth rate has become steady,  $Rm > Rm_2$  (see Figure 5).

## 5 Asymptotic behavior

We have finally increased the control parameter in the range 215–25000. Despite the fact that the largest magnetic Reynolds number tackled in this study is roughly 15 times larger than earlier results, the growth rate has not reached an asymptotic value yet. The growth rate obtained for our largest  $Rm$  is very close to 0.1 and appears to be still increasing with  $Rm$ .

The 1 : 1 : 1 ABC-flow has also been considered by Gilbert (1992) using maps in a limit in which the diffusivity is formally set to zero. This approach has yield growth rate of 0.04 – 0.05, so much smaller than the value achieved by our direct numerical simulations at  $Rm = 25000$ . It is therefore not unplausible to anticipate that the behavior of  $\sigma(Rm)$  above 25000 will not be monotonic and  $\sigma$  will probably decrease again.

Another indication is provided by the largest Lyapunov exponent of the flow, which is approximately 0.055 (see Galanti, Sulem, and Pouquet (1992)). Howing to the lack of regularity of the field in he limit of large  $Rm$  numbers, the largest Lyapunov exponent however does not provide an upper bound on the asymptotic growth rateChildress and Gilbert (1995). An upper bound can be sought by considering the topological entropy  $h_{\text{top}}$  (see Finn and Ott (1988a,b)). For steady three-dimensional flows the topological entropy is equal to the line stretching exponent  $h_{\text{line}}$  (see Childress and Gilbert (1995)), which can be estimated for the 1 : 1 : 1 ABC-flow to be  $h_{\text{line}} \simeq 0.09$ . This provides yet another indication that the curve  $\sigma(Rm)$  must decrease for larger values of  $Rm$ .

This unexpectedly rich behavior of the 1 : 1 : 1 ABC-dynamo at very large  $Rm$  deserves

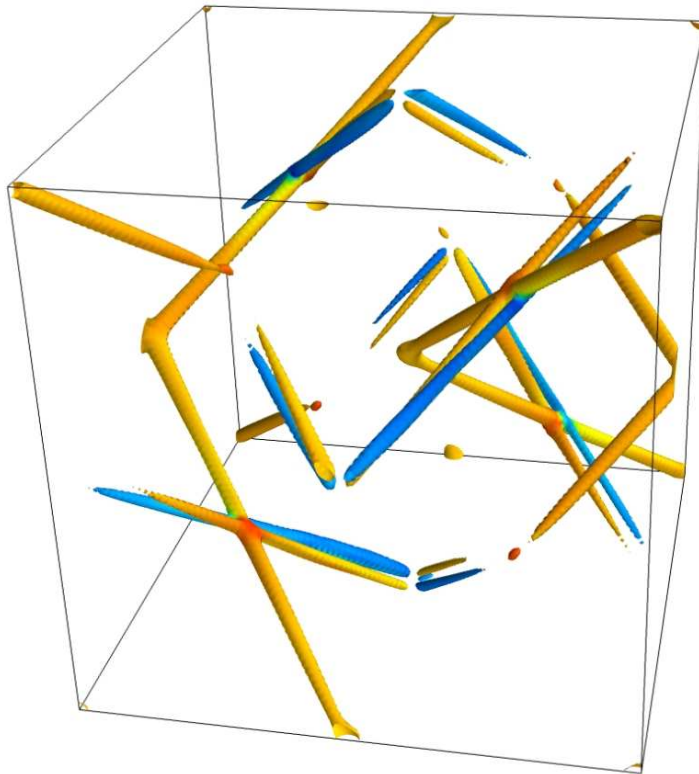


Figure 5: Eigenmode obtained for  $Rm = 434.2 (> Rm_2)$ . An isosurface of the magnetic energy is represented. To highlight the symmetry, it is colored according to the value of  $B_x$ , from blue (negative) to red (positive). The corresponding eigenvalue is purely real, yet the double cigars structure of the field remains clearly visible.



further investigations. It highlights the fact that this choice of parameters yields very small chaotic regions and is not optimal from the point of view of fast dynamo Galloway (2012). In particular to assess whether this non-monotonic behavior of the growth rate is associated further with changes in the symmetry of the dominant eigenmode (see Gilbert (1992) for discussion of possible symmetries).

## Acknowledgements

The authors are very grateful to Dave Galloway for sharing his original dynamo code, which served as the starting point for the parallel version written for this study.

Computations were performed using the mesospl cluster and the cines computing center (project Ira0633).

## References

- T. Dombre, U. Frisch, J. Greene, M. Henon, A. Mehr, and A. Soward, “Chaotic streamlines in the ABC flows,” *J. Fluid Mech* **167**, 353–391 (1986).
- V. Arnol’d, Y. Zel’dovich, A. Ruzmaikin, and D. Sokolov, “Magnetic field in a stationary flow with stretching in riemannian space,” *Sov. Phys.-JETP (Engl. Transl.);(United States)* **54** (1981).
- S. Childress and A. Gilbert, *Stretch, twist, fold: the fast dynamo* (Springer, 1995).
- V. Arnold and E. Korkina, “The growth of a magnetic field in the three-dimensional steady flow of an incompressible fluid,” *Moskovskii Universitet Vestnik Serii Matematika Mekhanika* **1**, 43–46 (1983).
- D. Galloway and U. Frisch, “A numerical investigation of magnetic field generation in a flow with chaotic streamlines,” *Geophysical & Astrophysical Fluid Dynamics* **29**, 13–18 (1984).
- D. Galloway and U. Frisch, “Dynamo action in a family of flows with chaotic streamlines,” *Geophysical & Astrophysical Fluid Dynamics* **36**, 53–83 (1986).
- D. Galloway and U. Frisch, “A note on the stability of a family of space-periodic beltrami flows,” *Journal of Fluid Mechanics* **180**, 557–564 (1987).
- V. Arnold, “Sur la topologie des écoulements stationnaires des fluides parfaits,” *CR Acad. Sci. Paris* **261**, 17–20 (1965).
- M. Henon, “Sur la topologie des lignes de courant dans un cas particulier,” *CR Acad. Sci. Paris* **262**, 312–314 (1966).
- V. Archontis, S. Dorch, and Å. Nordlund, “Numerical simulations of kinematic dynamo action,” *Astronomy and Astrophysics* **397**, 393–399 (2003).

- A. Alexakis, “Searching for the fastest dynamo: Laminar ABC flows,” *Physical Review E* **84**, 026321 (2011).
- D. Galloway, “ABC flows then and now,” *Geophysical & Astrophysical Fluid Dynamics* **in press** (2012), 10.1080/
- Y. Lau and J. Finn, “Fast dynamos with finite resistivity in steady flows with stagnation points,” *Physics of Fluids B: Plasma Physics* **5**, 365 (1993).
- R. Teysier, S. Fromang, and E. Dormy, “Kinematic dynamos using constrained transport with high order godunov schemes and adaptive mesh refinement,” *Journal of Computational Physics* **218**, 44–67 (2006).
- S. Dorch, “On the structure of the magnetic field in a kinematic ABC flow dynamo,” *Physica Scripta* **61**, 717 (2000).
- A. Gilbert, “Magnetic field evolution in steady chaotic flows,” *Philosophical Transactions of the Royal Society of London. Series A: Physical and Engineering Sciences* **339**, 627–656 (1992).
- B. Galanti, P. Sulem, and A. Pouquet, “Linear and non-linear dynamos associated with ABC flows,” *Geophysical & Astrophysical Fluid Dynamics* **66**, 183–208 (1992).
- J. Finn and E. Ott, “Chaotic flows and fast magnetic dynamos,” *Physics of Fluids* **31**, 2992 (1988a).
- J. Finn and E. Ott, “Chaotic flows and magnetic dynamos,” *Physical review letters* **60**, 760–763 (1988b).